

# Embankment evolution of a gravel road on permafrost terrain five years after construction: The Inuvik-Tuktoyaktuk Highway

Jennifer Kayley Humphries<sup>1</sup>, Jurjen van der Sluijs<sup>2</sup>, Peter D. Morse<sup>3</sup>, & Steven V. Kokelj<sup>4</sup>

<sup>1</sup>*Aurora Research Institute, Aurora College, Inuvik, Northwest Territories, Canada*

<sup>2</sup>*NWT Centre for Geomatics, Government of Northwest Territories, Yellowknife, Northwest Territories, Canada*

<sup>3</sup>*Geological Survey of Canada, Natural Resources Canada, Ottawa, Ontario, Canada*

<sup>4</sup>*Northwest Territories Geological Survey, Government of Northwest Territories, Yellowknife, Northwest Territories, Canada*



## ABSTRACT

The Inuvik-Tuktoyaktuk Highway (ITH) is a 137-km gravel road constructed during winters 2014–17 using frozen materials from seven borrow sources for a fill-only embankment designed to protect underlying permafrost. Road-surface settlement has occurred with active layer development and consolidation, compounded by right-of-way edge effects. To explore the evolution of a gravel road embankment on permafrost five years after construction we: 1) examine active layer development in the road and undisturbed terrain; 2) assess embankment thicknesses by differencing 2021 Lidar elevations with the 2011 pre-construction terrain; and 3) summarize field observations of underlying ice-wedge thaw and remotely-sensed rates of road-surface subsidence. In 2021, embankment centerline thaw depths approximated using ground temperature data were estimated to range from 2.3 to 3.7 m, which exceeded seasonal thaw depths in the adjacent tundra by 5-fold. The Lidar-derived embankment thicknesses in 2021 were less than 1.5 m for about 58% of the road length, suggesting that the embankment may be thawed by the end of summer for approximately half of the road length. Ice-wedge subsidence recorded at 57 locations, was associated with thin embankments and more frequent in the northern half of the corridor, excluding the last 25 km where the ITH was constructed on a pre-existing borrow pit access road that likely thawed near-surface permafrost before ITH construction. Estimated road surface subsidence from the period August 2019 to August 2021 supports these patterns. The findings demonstrate the value of systematic collection and analyses of monitoring data on road-permafrost interactions to inform design and maintenance that maximizes safety and performance.

## 1 INTRODUCTION

The Inuvik-Tuktoyaktuk Highway (ITH) connects Tuktoyaktuk, NWT on the Arctic Coast with Inuvik, NWT, and the rest of the National Highway System (Figure 1). Construction of the 137 km-long highway began in 2014 and it was officially opened on November 15, 2017. The road traverses complex, ice-rich permafrost terrain (Rampton 1988). To minimize ground disturbance and preserve underlying permafrost the highway was designed as a fill-only embankment constructed with frozen granular materials in winter. Construction of the highway sourced materials from seven borrow pits along the route. Materials were of variable quality, composed of unconsolidated silt, sand, and gravel sediment with significant ice content (Castagner et al. 2022). It was expected that the roadbed would settle (consolidate) in the first several years following construction, requiring maintenance efforts during this time. Road design accounted for variations in the terrain and ground ice conditions and established a minimum thickness necessary for various terrain types to protect the underlying permafrost (Grozić and Zhang 2018). Degradation of permafrost occurs when seasonal thaw is greater than the combined thickness of the embankment and pre-construction active layer. Under thick embankments and with favorable climate conditions, permafrost may aggrade into the embankment. Informed by geotechnical

investigations and ground-thermal data collected along the proposed alignment, thermal analyses were undertaken to estimate the maximum thaw depth into the road embankment under various ground and climate conditions. 2-D analyses were performed to assess temperature distributions for selected road and embankment geometries (Grozić and Zhang 2018). Minimum road height was determined to be 1.7 to 2.0 m of embankment material depending on the terrain, plus 200 mm of surface gravel (EGT Northwind 2013). Construction of the road began from the communities of Inuvik and Tuktoyaktuk and progressed towards the middle. Due to budgetary constraints, the decision was made to reduce the quantity of material for the project and reduce the embankment height for the 56 km of the road (km 20 to 76) that had not yet been constructed by the final year (CBC News 2016). The minimum embankment height was reduced to 1.2 m for the portions of the road between km 20 to 76 that were considered favorable low-risk terrain. Grozić and Zhang (2018) provided an overview of ITH construction and thaw depth development one season after road opening and described some reasons why thaw depths in 2017 were greater than those from the pre-design geothermal analysis, including thaw-consolidation of the road embankment and uncharacteristically warm summer temperatures. In conjunction with continued climate warming, variable snow accumulation, and challenges with drainage and ponding



Figure 1. ITH right of way and road surface disturbances. (a) km 100: A linear depression and sinkhole caused by ice wedge thaw and surface subsidence. (b) km 46: An aerial view of ice wedge subsidence beneath the highway embankment, with the thin arrows indicating degraded troughs and thick arrows indicating degraded troughs with ponds at the embankment edge. (c) km 106: Ponding, embankment sloughing, degrading ice wedges, and a heaved mat of organic materials from a large icing and frost blister that developed in the winter 2020/21. (d) km 94: Ice wedges beneath the road expressed as subtle linear depressions, indicated by grey dashed lines, and associated degradation and ponding of ice wedges adjacent to the road. Photos by GNWT – Jurjen van der Sluijs, August 2022 (a), Aurora College – Celtie Ferguson, September 2023 (b), and June 2021 (c), and Aurora College – Jen Humphries, September 2023 (d).

along the embankment edge, the thermal and physical conditions characterizing the ITH embankment can be expected to continue evolving with implications for road performance and maintenance (Figure 1).

Collaboration of government and community partners, and investment in local monitoring capacity have enabled the establishment of an ITH thermistor network, the completion of post-construction airborne Lidar and drone topographic

surveys (van der Sluijs et al. 2018, 2023; Ensom et al. 2020), and the development of a basic field survey to track road conditions and permafrost interactions.

This paper investigates the thermal and physical characteristics of the ITH embankment five years after construction and summarizes some indicators of permafrost thaw beneath the embankment. Specifically, we: 1) present thermal data to examine the range of thaw depths

measured in the road and undisturbed terrain; 2) assess 2021 embankment thicknesses by differencing 2021 Lidar elevations with the 2011 pre-construction terrain; 3) summarize settlement from 2019 to 2021 for embankments of different thicknesses; and 4) present a survey of road-surface subsidence correlating to ice-wedge thaw. These data and results support a discussion of the thermal and physical evolution of a gravel road over permafrost terrain 5 years after construction, and the value of sustained thermal and observational monitoring to inform future design and to support asset management and maintenance planning.

## 1.1 Study Area

The ITH forms a 137 km corridor across the forest-tundra transition zone and is underlain by ice-rich permafrost (Figure 2; Burn and Kokelj 2009). Cooler and drier conditions near the coast and warmer and wetter conditions inland are accompanied by the transition from shrub tundra to taiga forest (Lantz et al. 2013). A northward decrease in ground temperatures is associated with lower thaw season temperatures and thinner snow cover towards the coast (Kokelj et al. 2017).



Figure 2. The ITH corridor and locations of the 23 ground temperature monitoring sites. This includes 10 “Sentinel” sites in natural environments, and 13 “Embankment” sites distributed across treeline (dashed green line) from 14 to 81 km north on the ITH. NTGS 10 is a tundra hilltop at km 120.

The ITH corridor passes through two primary physiographic regions; the Anderson Plain in the south and the Tuktoyaktuk Coastlands in the north (Rampton 1988). The region was glaciated during the late Wisconsinan and surficial materials are predominantly fine-grained tills

making up the rolling hills, and glaciolacustrine deposits overlain by peatlands in lower-lying areas. The southern part of the corridor is characterized by gently rolling terrain comprising moraine and colluvial deposits. The Tuktoyaktuk Coastlands to the north are a low-elevation till plain with many ice-cored hills composed of glaciofluvial sands (outwash plains and ice contact deposits) and broad lacustrine plains (Rampton 1988). The permafrost throughout the region is ice-rich, with near-surface aggradational ice common in the upper 2–3 m of ground (Kokelj and Burn 2003). Segregated intrusive ice is more common in the northern part of the corridor in association with ice contact and outwash deposits (Rampton 1988). Ice wedges occur in organic deposits throughout the region, but they become larger and more widespread north of the tall shrub transition zone, where lacustrine basins and polygonal peatlands become a dominant landscape element (Figure 1; Mackay 2000; Kokelj et al. 2014). This undulating and poorly-drained environment is also lake-rich, with a greater abundance of waterbodies in the northern half. A high density of lakes and ponds in conjunction with ice-rich and often undulating terrain produce complex landscapes for road design, with large volumes of fill required to avoid cutting slopes. This water-rich environment required the construction of 8 bridges and over 300 culverts to convey creeks, ephemeral streams, and slope runoff past the embankment. Materials were excavated in a frozen state and it was expected that the roadbed would consolidate as the active layer developed in the embankment through the first several years following construction.

Mean annual air temperature (MAAT) for the 1981–2010 period was  $-8.2^{\circ}\text{C}$  and  $-10.1^{\circ}\text{C}$  in Inuvik and Tuktoyaktuk, respectively (Environment Canada 2023). Over the same period, the mean total precipitation in Inuvik was 241 mm, of which 159 mm fell as snow, and 161 mm, with 103 mm as snow, in Tuktoyaktuk (Environment Canada 2023). Mean annual ground temperature (MAGT) near Inuvik ranges from  $0^{\circ}\text{C}$  to  $-4^{\circ}\text{C}$ , and decreases to minimum temperatures of about  $-7^{\circ}\text{C}$  near Tuktoyaktuk (Kokelj et al. 2017). Climate change is driving rapid increases in air and ground temperatures, with Burn and Kokelj (2009) reporting MAGT rising by about  $2^{\circ}\text{C}$  from the 1970s to the 2010s in the Mackenzie Delta region. A wide range of permafrost temperatures and high ground ice content, particularly in the form of ice wedges and relict ice, along the ITH indicate permafrost is susceptible to thawing or degradation from climate warming, alterations to surface conditions such as snow or vegetation, and by way of disturbances such as ponding, thermal erosion, and construction (Kokelj et al. 2017; Burn et al. 2009). In the case of the ITH, rapid regional warming is occurring in concert with alterations to snow and vegetation conditions and disturbances introduced by the development of the highway.

## 2 METHODOLOGY

### 2.1 Permafrost

Ground temperature data were collected as part of two collaborative monitoring programs – the “Sentinel sites”, and the “ITH Embankment sites” (Ensom et al. 2020). The

Sentinel network comprises undisturbed hilltop, peatland, and riparian environments as well as borrow pits along the ITH corridor, while the ITH Embankment sites include boreholes through a range of embankment thicknesses from km 23 to 120 (Figure 2). The Sentinel sites analyzed in this paper (Table 1) are in undisturbed tundra ranging from 40 to 360 m away from the ITH. The 14 ITH Embankment sites were instrumented in 2017, each with a single ground temperature cable (GTC). One site, ITH 3, was destroyed early on so only 13 sites were used for the analysis (Table 1). Boreholes were drilled through the embankment and a minimum of 2 m into the native soil. GTCs were installed vertically through the embankment, and horizontally along a shallow trench to the shoulder of the road. Only the centreline data was used for this study. The total borehole depths of the GTCs ranged from 3.0 to 6.7 m. Each Embankment GTC consisted of 13 YSI #44007 thermistor beads and a Lakewood RX16 data logger. Full details on the installation of ITH Embankment sites and ground temperature data are available in Rudy et al. (2020a,b).

Table 1. Site IDs, associated project, generalized site type and occurrence of disturbance for each site.

Site IDs	Project	Site type	Disturbance
ITH 1,2, 4-14	ITH Embankment	Embankment	Disturbed
NTGS 1-10	Sentinel	Tundra	Undisturbed

\* ITH 2 and 3 were destroyed, but ITH 2 had a record of <2 years

\* NTGS 6 only has a shallow instrument (1.5 m), and NTGS 10 was installed to a depth of 13.5 m

As part of the Sentinel project in 2017, 16 sites were originally instrumented (NTGS 1–13, 15–17), each with a deep and shallow GTC. Only data from NTGS 1–10 were used in this study as they represent conditions in undisturbed terrain; NTGS 11–13 and 15–17 represent disturbed terrain in borrow pits, and adjacent to a thaw slump. The deep boreholes were drilled to a depth of either 10 or 20 m and were instrumented with five or six GeoPrecision PT1000 sensors and an M-Log5W data logger. The shallow GTCs were installed within 5 m of the deep GTC to a depth of 1.5 m, and were instrumented with four thermistors (Onset TMC6-HD) at 0.2, 0.5, 1.0 and 1.5 m below the surface and a four-channel HOBO U12-008 data logger. Full details of the installation and the first year of data collection at the Sentinel sites are available in Rudy et al. (2020c,d).

In total, data from 23 sites were analyzed; 13 Embankment sites with one GTC, and 10 Sentinel sites with paired deep and shallow GTCs. Daily average ground temperatures were used for examining the ground thermal regime at the 23 sites. To use the available data record, years were defined as 365-day periods beginning on October 16, 2017 and ending on October 15, 2022 (e.g., 2017–18 year covers from October 16, 2017 to October 15, 2018, and the 2021–22 year includes October 16, 2021 to October 15, 2022). The daily maximum, minimum, and average ground temperatures were calculated for each year. If there were less than 365 daily temperature values, the values were manually added or discarded. Maximum thaw depth is the depth of maximum penetration of the 0°C isotherm (Burn 1998). In a ground temperature envelope, it is the maximum

depth at which the maximum daily temperature rises above 0°C. At each site, the maximum thaw depth was approximated for each year by determining where the linearly interpolated line between two thermistor depths crossed the 0°C isotherm. Thermistor depths in the embankments are reported relative to the road surface at the time of installation in 2017. It is not known how much the embankment has settled in the 5 years from construction at thermistor locations, or how operation and maintenance activities have changed the thickness of the material cover, both of which may have impacted the relative position of the GTCs.

## 2.2 Road Elevation and Hazards

Airborne Light Detection and Ranging (Lidar) and photogrammetry data provided baseline elevation datasets. Lidar-derived DEMs (1-m spatial resolution) for August 2011 and August 2021 were used to generate a differencing product (DEM of Difference; DOD) after accounting for vertical datum differences. More details on the Lidar data and DOD methodology are available in van der Sluijs et al. (2018). The DOD, characterizing embankment thickness, was sampled every 100 m for the entire length of the road for graphing and analysis. Photogrammetry-derived DEMs collected in August 2019 by long-endurance drone for most of the highway (km 0 to km 127; van der Sluijs et al. 2023), and by Lidar in 2021 were used to determine road-surface subsidence between 2019 and 2021 at the same 100-m sampling interval. Here elevations were differenced to obtain 2-year subsidence estimates summarized by embankment thickness class (< 0.5 m, 0.5–1.5 m, > 1.5 m), after corrections were made for any systematic DEM offsets between the two DEMs at locations away from the road surface.

To gather systematic spatial information on permafrost-related road hazards, a digital field form hosted on ESRI Survey123 was developed. The ITH was surveyed in September 2022. The survey form collected three main pieces of information for each hazard: location (coordinates), position relative to the road (on the road or right of way), and type of hazard. The main hazards were: cracking, potholes, culvert issues, washboard, subsidence, ponding, and ice wedge degradation. The form was intended to gather information on the prevalence and location of permafrost-related road hazards, and not as a comprehensive inventory of road hazards and performance issues.

## 3 RESULTS

### 3.1 Permafrost temperatures

Ground temperature envelopes show that embankment sites have a much greater near-surface seasonal temperature variation than undisturbed tundra (Figure 3), due to the contrasting material properties and ground surface conditions (vegetation and snow) between the road embankment and natural tundra environment. In undisturbed tundra, minimum winter temperatures at 1.0 m depth ranged from -9.0°C to -16.6°C in 2021–22. At comparable depths below the centreline of the snow-free

granular embankment surface (0.9 to 1.1 m), minimum temperatures were much lower, ranging from -24.4 °C to -30.5 °C over the same period. The embankment also experienced much higher maximum summer temperatures, ranging from 11.4 °C to 22.1 °C between 0.9 and 1.1 m depth, whereas maximum temperatures at 1.0 m in natural terrain ranged from -0.9 °C to 0.1 °C. The strong connection between air and road surface temperatures is reflected in high freezing and thawing n-factors (Stockton et al. 2024). As a result of these distinct ground thermal conditions, active layer thicknesses in the roadbed were more than 4 times greater than in the adjacent tundra, with medians of 2.9 m and 0.7 m, respectively (Figure 3; Table 2). In the top 5 m of ground, winter minimum temperatures in tundra and the embankment were lower in 2021–22 than in 2017–18. Maximum temperatures were similar between the two years of record at tundra sites, but at embankment sites indicate the maximum depth of thaw was greater in 2021–2022. The most significant implication of the large embankment thaw depths is the potential degradation of permafrost underlying the road.

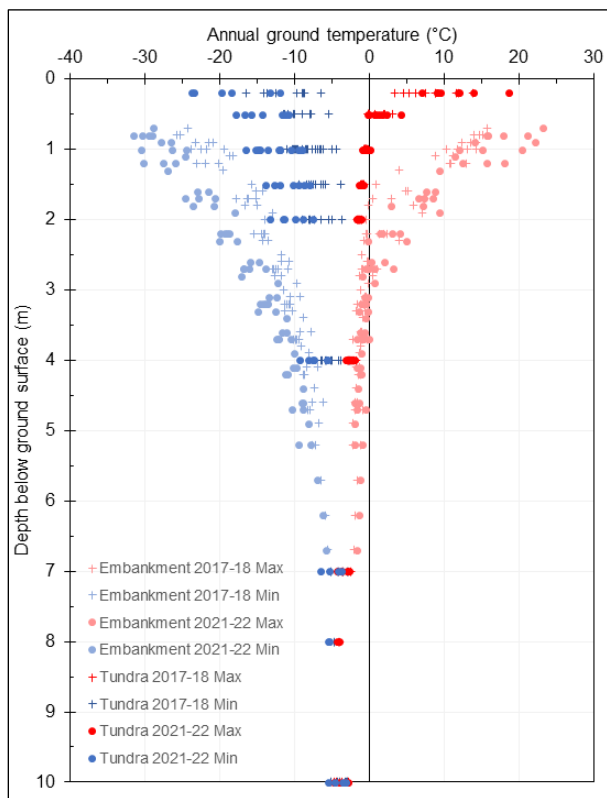


Figure 3. Ground temperature envelopes for 2017–18 and 2021–22, showing maximum and minimum daily temperatures with depth. Shaded colours are the embankment sites (ITH 1–2, 4–14), and solid colours are the tundra sites (NTGS 1–10). Depths for embankment sites are relative to the road surface at the time of installation in March 2017.

There is an inverse relationship between embankment thickness and thawing of the underlying native ground inferred from the temperature data at the 10 ITH boreholes

(Figure 4). Assuming (1) the maximum active layer thickness in the original terrain that the highway was built over was between 0.5 and 1.0 m (Table 2), and (2) considering the thermistor depths relative to the original ground surface, we can estimate whether permafrost has aggraded or degraded under different embankment thicknesses (Figure 4). Maximum thaw depths relative to the 2017 embankment thicknesses at the 13 sites suggests that in all but one deep-fill embankment site, thaw depths in 2022 reach below the original ground surface. This is confirmed by the shallowest thermistor in native soils beneath the embankment which rise above 0 by end of summer 2022 for 10 out of 12 sites with available data (Table 2). The thickest embankment (4.6 m), and the greatest thaw depth (3.7 m; Table 2) were found at ITH 10; it was also the only site where thaw depth was maintained within the embankment materials above the original ground surface (Figure 4). At 7 sites with embankments between 1.5 and 2.7 m maximum thaw depths were estimated to be within the active layer of the preconstruction terrain (Figure 4). At 4 sites with embankment thicknesses of less than 1.5 m, the thaw depths exceed the thickness of the road embankment and the original active layer resulting in some permafrost degradation.

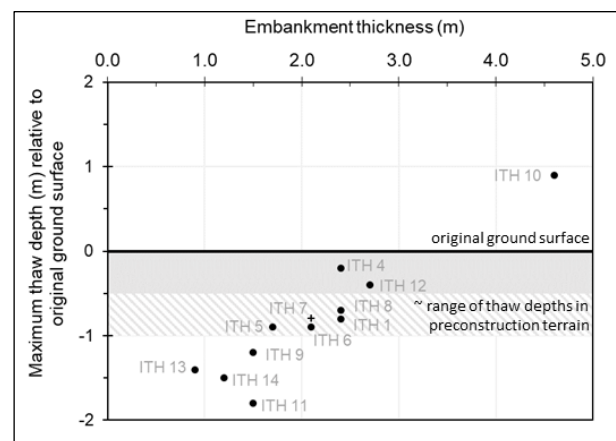


Figure 4. Estimated thaw depths at embankment sites relative to the original ground surface (i.e., native ground) against constructed embankment fill thickness in 2017. The grey box represents the preconstruction active layer zone and the hatched area approximates the position of the permafrost table in preconstruction terrain. Black dots indicate thaw depths from 2021–22; + indicate data from 2020–21.

### 3.2 Road Condition

Consolidated centerline embankment thickness estimated by differencing preconstruction and August 2021 Lidar, sampled at 100 m intervals, suggests that about 42% of the ITH embankment is > 1.5 m thick (Figure 5a). Although numerous deep fills occur along the highway length, the greatest abundance of thick embankments are between km 0 and km 20, and between km 105 and about km 120—the ends of the highway that were constructed early on in the project using the original design heights (see section 1), and where deep fills were required to negotiate complex

topography (Figure 5b). The DOD product suggests that in August 2021, 58% of the highway had a thickness of less than 1.5 m, and 16% had a thickness of less than 0.5 m. Based on maximum thaw depths inferred from embankment thermistor data (Table 2), it can be conservatively estimated ground beneath embankments less than 1.5 m thick thaws annually, and that the original permafrost has begun to thaw beneath embankments less than 0.5 m thick.

Table 2. Mean annual ground temperature (MAGT) near 1 m depth, estimated active layer thickness, and an indication of whether the uppermost thermistor below the embankment (native ground) thawed at sites along the ITH 2021-22.

Site	Thickness (m)	km	MAGT (°C)	MAGT Depth (m)	Active layer (m)	Embankment thawed (Y/N)
ITH 1	2.4	23	-5.1	0.9	3.1	Y
ITH 2	0.9	28	—	0.9	—	—
ITH 4	2.4	32	-6.4	0.8	2.6	Y
ITH 5	1.7	35	-6.0	1.0	2.6	Y
ITH 6	2.1	43	-6.1	0.9	3.0	Y
ITH 7	2.1	44	-5.8*	1.1	2.9*	Y*
ITH 8	2.4	47	-6.0	1.1	3.1	Y
ITH 9	1.5	51	-5.9	1.0	2.7	Y
ITH 10	4.6	57	-5.7	1.0	3.7	N
ITH 11	1.5	60	-5.6	1.0	3.3	Y
ITH 12	2.7	65	-6.2	0.8	3.1	N**
ITH 13	0.9	69	-6.0	0.8	2.3	Y
ITH 14	1.2	72	-6.3	0.8	2.7	Y
<b>Embankment</b>					<b>2.9</b>	
NTGS 1		14	-4.4*	1.0	0.8	
NTGS 2		14	-3.7	1.0	0.9	
NTGS 3		14	-3.9	1.0	0.5	
NTGS 4		42	-5.3*	1.0	0.5	
NTGS 5		42	-5.6	1.0	0.9	
NTGS 6		43	-4.3*	1.0	0.5	
NTGS 7		82	-4.0	1.0	1.0	
NTGS 8		81	-6.0	1.0	0.8	
NTGS 9		80	-4.5	1.0	0.7	
NTGS 10		120	-4.6*	1.0	0.8	
<b>Tundra</b>					<b>0.7</b>	

\* data from 2020-21

\*\* Thermistors in native soils range from 0.1 to 0.6 m depth. At ITH 12 thermistor is at 0.5 m depth.

An observational survey of thaw-induced hazards on and adjacent to the ITH was conducted in September 2022. The survey identified 57 locations where roadbed subsidence indicated the degradation of an underlying ice wedge (Figures 2a,b,d, and 5). Most of these occurrences were north of km 40, and were clustered on tundra uplands between Trail Valley and Hans Creeks (km 40 to km 55)—where the embankment was constructed to a reduced height—and in low-lying lacustrine plains with extensive polygonal peatlands between about km 80 and km 115. Although ice wedges are large and abundant near Tuktoyaktuk, there was only one observation of ice-wedge thaw directly affecting the northernmost portion of the ITH, constructed overtop of the pit 177 access road established in 2013. Within the context of these regional patterns, the highest density of ice-wedge subsidence expressed at the road surface (0.7 km<sup>-1</sup>) was associated with embankments < 0.5 m thickness, and the lowest density (0.14 km<sup>-1</sup>) was associated with embankments greater than 1.5 m thick.

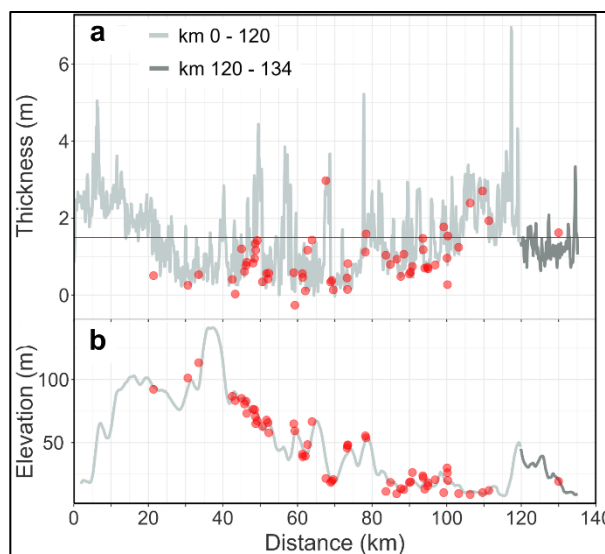


Figure 5. Longitudinal profiles along the ITH. (a) Profile of estimated embankment thickness in August 2021, and locations with evidence of ice-wedge thaw (red circles) in September 2022. The red horizontal line indicates an embankment thickness of 1.5 m. (b) Profile of terrain elevation along the road corridor, and evidence of ice-wedge thaw (red circles). Estimated embankment thicknesses were reported at 100 m intervals. The dark grey profile is the section of ITH constructed overtop of the source 177 access road.

Estimated road surface subsidence from the period August 2019 to August 2021 corroborates these patterns. Figure 6a shows that the thinnest embankments (< 0.5 m) experienced the greatest amounts of subsidence between 2019 and 2021, and those greater than 1.5 m thickness experienced little to no net elevation change (Figure 6). This pattern, in conjunction with evidence of ice-wedge thaw subsidence that was often associated with < 0.5 m embankments, supports the idea that ice-rich permafrost is thawing beneath the thinnest embankments (Figure 5), and that permafrost has either not thawed, or aggraded, beneath embankments that remain greater than 1.5 m thick. In stark contrast, net surface subsidence was not detected by this analysis for the northernmost section of the ITH, constructed over the pit 177 access road, regardless of embankment thickness.

#### 4 DISCUSSION

The estimated maximum thaw depths beneath the road surface (13 sites) 5 years following the completion of construction (Table 2) were on average 2.2 m greater than in undisturbed tundra (10 sites). The inferred active layer thicknesses in the road embankment estimated relative to the 2017 road surface ranged from 2.3 to 3.7 m. However, thaw consolidation and road maintenance activities such as grading, could decrease the road surface elevation, reducing the thickness of overburden between the surface and thermistors at depth resulting in an overestimation of true active layer thickness. Regardless, thermistors within

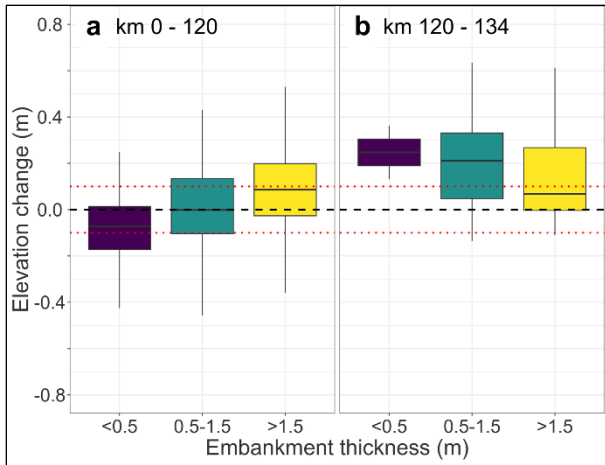


Figure 6. Box and whisker plots showing the net change in elevation of the road surface edge between August 2019 and August 2021, sampled at 100 m intervals along the ITH. Relative change stratified by embankment thickness is shown for (a) km 0 to km 120, and (b) km 120 to km 134. Red dashed line represents estimated level of uncertainty (10 cm) inferred from averaged standard deviation of elevations between the two DEMs at locations away from the road surface.

native soils below the embankment confirm that the embankment thaws at all sites with an original embankment thickness of less than 2.4 m (Table 2).

This preliminary examination of the embankment thermal data highlights the importance of monitoring thermistor cables and analyzing the data following construction because they can inform the revision of monitoring methods, and following more robust thermal analysis, enable engineers, designers, and planners to refine the assumptions and parameterization of thermal models to enhance the design of future roads. In particular, opportunities to examine thermal data and road performance may reinforce the value of conservative modeling estimates and design parameters in the context of warming air temperatures, and changing precipitation patterns. Furthermore, systematic collection of infrastructure conditions and geohazards, both on the road and within the right-of-way can guide maintenance plans.

Embankment thickness from 2021 Lidar showed 58% of the highway embankment is less than 1.5 m thick. Thin embankments are especially common between km 20 and km 100, in part due to the reduction of minimum embankment heights below design specifications during the later stages of construction. Patterns of change in road surface elevations and observations of ice-wedge subsidence suggest that permafrost beneath the thinnest embankments has begun to thaw.

Road settlement is the combined product of material quality, its ice content, level of compaction, surface grading, and the interactions of snow and water accumulation along the edge of the embankments. Once thaw exceeds embankment thickness and reaches the underlying permafrost, degradation of ice-rich ground can further

increase settlement. The observations reported in this study reinforce the need for a conservative design with thick embankments, and the potential permafrost implications of deviating from design. Construction of the most northerly portion of the ITH was staged by building over the pit 177 access road, which appears to have benefited the performance of the road. The pit 177 access road likely pre-thawed underlying ice-rich ground resulting in lower rates of settlement and little evidence of underlying ice-wedge thaw. Given the observations in this study that indicate the likely thawing of ice-rich permafrost underlying the ITH embankment, the complex interactions between changing right-of-way conditions, and a rapidly warming climate, systematic thermal and observational monitoring, and resources for data analysis to inform maintenance and mitigation measures are more important than ever.

## 5 CONCLUSIONS

Examining the thermal and physical characteristics of the embankment, five years following the construction of the Inuvik-Tuktoyaktuk Highway (ITH) several conclusions can be drawn:

- (1) Estimated thaw depths in the embankment are 2.3 to 3.7 m at 13 monitoring sites and exceed embankment thicknesses at 12 of the 13 sites. Temperatures in native ground beneath the embankment confirm that the embankment thawed by end of summer at all but the two thickest fill sites;
- (2) Based on a conservative approximation of embankment thaw depths and embankment thicknesses in 2021 it is estimated that the ITH embankment thaws by the end of summer along about 58% of its length;
- (3) The pattern of road surface settlement between 2019 and 2021, and observations of road surface subsidence caused by ice wedge thaw indicate that permafrost beneath the thinnest embankments has begun to thaw; and
- (4) The results indicate the value of systematically collecting and analyzing monitoring data along infrastructure corridors. The monitoring results can be used to assess road performance and inform future design of roads constructed over ice-rich permafrost.

## 6 ACKNOWLEDGEMENTS

This research has been supported by: Transport Canada's National Trade Corridors Fund (NTCF); Aurora Research Institute (ARI), Aurora College; Northwest Territories Geological Survey (NTGS), Government of Northwest Territories; NWT Centre for Geomatics, Government of Northwest Territories; Geological Survey of Canada (GSC); Inuvialuit Land Administration and Department of Infrastructure, Government of Northwest Territories. The authors are grateful to Kelly Kamo-McHugh and Richard Blake for collecting and providing ground temperature data, as well as staff from the NTGS, GSC, ARI, and Wilfrid Laurier University who have assisted with data collection

over the years. Helpful discussion with Ed Grozic and comments from two anonymous reviewers greatly improved the quality of this manuscript.

## 7 REFERENCES

- Burn, C.R. and Kokelj, S.V. 2009. 'The environment and permafrost of the Mackenzie Delta area', *Permafrost and Periglacial Processes* 20(2), pp. 83–105. doi:10.1002/ppp.655.
- Burn, C.R., Mackay, J.R., and Kokelj, S.V. 2009. 'The thermal regime of permafrost and its susceptibility to degradation in upland terrain near Inuvik, NWT', *Permafrost and Periglacial Processes* 20, pp. 221–227. doi: 10.1002/ppp.649.
- Castagner, A., Kokelj, S.V., and Gruber, S. 2022. 'A Cryostratigraphic Synthesis of Inuvik to Tuktoyaktuk Highway Corridor Geotechnical Boreholes (2012–2017)', NWT Open Report 2022-002, 12 pp. + appendix.
- CBC News 2016. 'Remaining Inuvik-Tuk highway to use less gravel to save money'. *CBC News* January 19, 2016. Available at: <https://www.cbc.ca/news/canada/north/inuvik-tuktoyaktuk-highway-gravel-1.3411200>.
- EGT Northwind Ltd., Kavik-Stantec Inc., and Kiggiak-EBA Consulting Ltd. [EGT Northwind] 2013. *Design Report–Inuvik to Tuktoyaktuk Highway: 100% Geometric and Structures Design*. Prepared for Department of Transportation, Government of Northwest Territories, 299 pp.
- Ensom, T.E., Kokelj, S.V., Morse, P.D., and Kamo McHugh K. 2020. 'Permafrost Ground Temperature Data Synthesis: 2013-2019 Inuvik-Tuktoyaktuk Highway region, Northwest Territories', *Northwest Territories Geological Survey NWT Open Report* 2019-020, 13 pp. + appendix.
- Environment Canada 2023. *Canadian Climate Normal 1981–2010 station data*. Available at: [https://climate.weather.gc.ca/climate\\_normals/index\\_e.html](https://climate.weather.gc.ca/climate_normals/index_e.html) [Accessed: 1 August 2023].
- Grozic, E. and Zhang, G. 2018. 'Inuvik to Tuktoyaktuk Highway Road Embankment Constructed on Ice-Rich Permafrost Terrain', in *Proceedings of GeoEdmonton 2018*, Edmonton, Alberta, Canada. Available at: <https://members.cgs.ca/conferences/GeoEdmonton/index.html>.
- Kokelj, S.V. and Burn, C.R. 2003. 'Ground ice and soluble cations in near-surface permafrost, Inuvik, Northwest Territories', Canada', *Permafrost and Periglacial Processes* 14, pp. 275–289. doi:10.1002/ppp.458.
- Kokelj, S.V., Lantz, T.C., Wolfe, S.A., Kanigan, J.C., Morse, P.D., Coutts, R., Molina-Giraldo, N., and Burn, C.R. 2014. 'Distribution and activity of ice wedges across the forest-tundra transition, western Arctic Canada', *Journal of Geophysical Research Earth Surface* 119, pp. 2032–2047. doi:10.1002/2014JF003085.
- Kokelj, S.V., Palmer, M.J., Lantz, T.C., and Burn, C.R. 2017. 'Ground Temperatures and Permafrost Warming from Forest to Tundra, Tuktoyaktuk Coastlands and Anderson Plain, NWT, Canada', *Permafrost and Periglacial Processes* 28, pp. 543–551. doi:10.1002/ppp.1934.
- Lantz T.C., Marsh, P., and Kokelj S.V. 2013. 'Recent shrub proliferation in the Mackenzie Delta Uplands and microclimatic implications', *Ecosystems* 16, pp. 47–59. doi:10.1007/s10021-012-9595-2.
- Mackay, J.R. 2000. 'Thermally induced movements in ice-wedge polygons, western arctic coast: a long-term study', *Géographie physique et Quaternaire* 54, pp. 41–68. doi: 10.7202/004846ar.
- Rampton, V.N. 1988. 'Quaternary Geology of the Tuktoyaktuk Coastlands, Northwest Territories', *Geological Survey of Canada Memoir* 423, 98 pp. doi:10.4095/126937.
- Rudy, A.C.A., Kokelj, S.V., and Ensom, T. 2020a. 'Permafrost Geotechnical Report: Inuvik to Tuktoyaktuk Highway Embankment Boreholes', *Northwest Territories Geological Survey NWT Open Report* 2019-011, 7 pp. + geotechnical data + appendix.
- Rudy, A.C.A., Kokelj, S.V., and Ensom, T. 2020b. 'Permafrost Ground Temperature Report: Inuvik to Tuktoyaktuk Highway Embankment Sites', *Northwest Territories Geological Survey NWT Open Report* 2019-016, 8 pp. + ground temperature data + appendix.
- Rudy, A.C.A., Kokelj, S.V., Morse, P.D., and Ensom, T. 2020c. 'Permafrost Geotechnical Report: Inuvik to Tuktoyaktuk Highway Sentinel Program Boreholes, Northwest Territories', *Northwest Territories Geological Survey NWT Open Report* 2019-008, 7 pp. + geotechnical data + appendix.
- Rudy, A.C.A., Kokelj, S.V., Morse, P.D., and Ensom, T. 2020d. 'Permafrost Ground Temperature Report: Inuvik to Tuktoyaktuk Highway Sentinel sites', *Northwest Territories Geological Survey NWT Open Report* 2019-017, 8 pp. + ground temperature data + appendix.
- van der Sluijs, J., Kokelj, S.V., Fraser, R.H., Tunnicliffe, J., Lacelle, D. 2018. 'Permafrost Terrain Dynamics and Infrastructure Impacts Revealed by UAV Photogrammetry and Thermal Imaging', *Remote Sensing* 10(11), 1734. doi:10.3390/rs10111734
- van der Sluijs, J., Saiset, E., Bakelaar, C.N., Wentworth, A., Fraser, R.H. and Kokelj, S.V. 2023. 'Beyond visual-line-of-sight (BVLOS) drone operations for environmental and infrastructure monitoring: a case study in northwestern Canada', *Drone Systems and Applications* 11, pp. 1–15. doi:10.1139/dsa-2023-0012.